JCTC Journal of Chemical Theory and Computation

Article

pubs.acs.org/JCTC

Gaussian Expansions of Orbitals

Laura K. McKemmish* and Peter M. W. Gill*

Research School of Chemistry, Australian National University, Canberra, ACT 0200, Australia

ABSTRACT: Using numerical calculations and analytic theory, we examine the convergence behavior of Gaussian expansions of several model orbitals. By following the approach of Kutzelnigg, we find that the errors in the energies of the optimal n-term even-tempered Gaussian expansions of s-type, p-type, and d-type exponential orbitals are $\varepsilon_n^{\mathrm{s}} \sim \exp(-\pi(3n)^{1/2})$, $\varepsilon_n^{\mathrm{p}} \sim \exp(-\pi(5n)^{1/2})$, and $\varepsilon_n^{\mathrm{d}} \sim \exp(-\pi(7n)^{1/2})$, respectively. We show that such "root-exponential" convergence patterns are a consequence of the orbital cusps at $r = 0$, rather than the over-rapid decay of Gaussians at large r. We find that even-tempered expansions of the cuspless Lorentzian orbital also exhibit root-exponential convergence but that this is a consequence of its fat tail.

1. INTRODUCTION

The concept of the molecular orbital (MO) lies at the heart of contemporary chemistry and is the central object in quantum chemistry.[1−4] Indeed, almost all of the understanding and rationalization in modern organic and inorganic chemistry is couched in terms of simple arguments involving the interactions between orbitals, particularly those near the HOMO−LUMO interface.[5−9]

For computational purposes, one must expand MOs in a set of basis functions,[10,11] and because of their unparalleled mathematical properties, Gaussian basis functions have been the pragmatic choice for many years. Because all of the integrals that arise in Hartree−Fock and traditional post-Hartree−Fock calculations can be reduced[12−27] to elementary functions and error functions,[28] Gaussians are ubiquitous in molecular calculations and have even challenged plane waves in solid-state calculations.[29,30]

However, from a theoretical viewpoint, Gaussians are suboptimal for two reasons: they lack a cusp[31] at $r = 0$, and they decay too fast[32] at large r. The complementary nature of these deficiencies becomes clear if an exponential function (the exact wave function for a hydrogen atom) and a Gaussian (the exact wave function for a harmonic oscillator) are superimposed as shown in Figure 1. The logarithmic transformation that converts the exponential into a straight line converts the Gaussian into a sigmoidal curve that is flat at both ends of the domain. It is obvious from Figure 1 that no finite linear combination of Gaussians can ever capture either the exponential cusp at $r = 0$ or the analogous "cusp" at $r = \infty$.

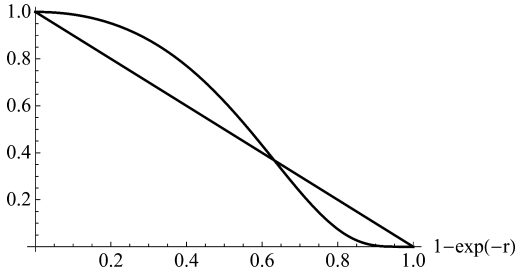

Figure 1. Comparison of $\exp(-r)$ and $\exp(-r^2)$ for $0 \le r < \infty$.

However, for an electron in a radial potential, one can construct the n-Gaussian wave function approximations

$$\psi_n = \sum_{i=1}^{n} c_i \exp(-\alpha_i r^2) \tag{1}$$

that minimize the energy expectation value

$$E_n = \min_{c,a} \frac{\langle \psi_n | H | \psi_n \rangle}{\langle \psi_n | \psi_n \rangle} \tag{2}$$

and study the convergence of the E_n to the true E. Huzinaga took this approach[33] to find the coefficients c_i and exponents α_i for the H atom, and Kutzelnigg and Klopper later used cardinal function theory[34] to show[35−39] that, if the α_i's are even-tempered[40,41] (i.e., they form a geometric sequence), the energy error $\varepsilon_n = E_n - E$ behaves asymptotically as

$$\varepsilon_n \sim \exp(-\pi\sqrt{3n}) \tag{3}$$

Root-exponential convergence is initially surprising, for spectral theory[34] leads one to expect algebraic convergence when a cusp is expanded in a basis of smooth functions. However, as Whittakers showed,[42,43] this expectation can be exceeded when the smooth functions themselves are optimized (via optimization of the α_i).

Do *both* of the cusp problems in Figure 1 lead to the root-exponential convergence (eq 3) of the H atom energy? Would this behavior persist if the exact wave function had only the $r = 0$ cusp, or only the $r = \infty$ cusp? These are key questions for understanding the fundamental issues that underlie the construction of efficient Gaussian basis sets, whether of the Pople,[44] Dunning,[45] or Jensen[46] type.

In this paper, we examine the Gaussian expansions of a variety of orbitals and present a general approach for predicting and rationalizing the rate of convergence of the energies of such expansions. We use atomic units throughout.

Special Issue: Berny Schlegel Festschrift

Received: July 3, 2012
Published: July 24, 2012

2. KUTZELNIGG ANALYSIS

We consider an electron, moving in a radial potential $V(r)$, with the radial[47] wave function $\psi(r)$ and energy E. If the full wave function has the angular momentum quantum number l, then the Gaussian representation[48] of the wave function

$$\psi(r) = r^l \int_0^\infty f(\alpha)\, \exp(-\alpha r^2)\, \mathrm{d}\alpha \tag{4}$$

can be viewed as its expansion as an infinite sum of Gaussians with exponents from $\alpha = 0$ to $\alpha = \infty$. However, it is even more illuminating to recast this in terms of the log-exponent $z = \ln \alpha$, thus obtaining

$$\psi(r) = r^l \int_{-\infty}^\infty g(z)\, \exp(-e^z r^2)\, \mathrm{d}z \tag{5}$$

The function $g(z)$ then measures the importance of the log-exponent z in the Gaussian expansion of $\psi(r)$ and, as we show below, foreshadows the range of exponents that contribute significantly in a *finite* expansion.

2.1. Energy Error Functional. If ψ is an exact eigenfunction of the Hamiltonian H, with eigenvalue E, then the energy error functional

$$\mathcal{E} = \langle \psi | H - E | \psi \rangle = \int_0^\infty \int_0^\infty F(\alpha, \beta)\, \mathrm{d}\alpha\, \mathrm{d}\beta \tag{6}$$

vanishes identically. The function

$$F(\alpha, \beta) = f(\alpha) f(\beta) \langle r^l \mathrm{e}^{-\alpha r^2} | T + V - E | r^l \mathrm{e}^{-\beta r^2} \rangle \tag{7}$$

decomposes $\mathcal{E}$ over Gaussian exponent space, revealing which exponents are important in the Gaussian expansion of ψ and which are less so. It is easy to show that

$$\int_0^\infty F(\alpha, \beta)\, \mathrm{d}\alpha = \int_0^\infty F(\alpha, \beta) \mathrm{d}\beta = 0 \tag{8}$$

(which we use in eqs 12 and 18) and that

$$F(\alpha, \beta) = f(\alpha) f(\beta) \left[\frac{(2l+3)\alpha\beta}{\zeta^{l+5/2}} + G(\zeta) - \frac{E}{\zeta^{l+3/2}} \right] \tag{9}$$

where $\zeta = \alpha + \beta$ and

$$G(\zeta) = \frac{2}{\Gamma(l+3/2)} \int_0^\infty V(r)\, \exp(-\zeta r^2) r^{2l+2}\, \mathrm{d}r \tag{10}$$

Approximating ψ by the finite Gaussian expansion (eq 1) is equivalent to truncating the integration domain in (eq 6) from $[0,\infty) \otimes [0,\infty)$ to $[L,U] \otimes [L,U]$ and then applying an n-point quadrature to each of the integrals, yielding

$$\mathcal{E} \approx \mathcal{E}_C + \mathcal{E}_D \tag{11}$$

Kutzelnigg refers to these two components as the "cutoff error" and "discretization error", respectively.

2.2. Cutoff Error. The vanishing of the integrals in eq 8 led Kutzelnigg to define the cutoff error as the sum

$$\mathcal{E}_C = \mathcal{E}_L + \mathcal{E}_U \tag{12}$$

of a lower cutoff error

$$\mathcal{E}_L \sim \int_0^L \int_0^L f_L(\alpha) f_L(\beta) \left[\frac{(2l+3)\alpha\beta}{\zeta^{l+5/2}} + G_L(\zeta) - \frac{E}{\zeta^{l+3/2}} \right] \mathrm{d}\alpha\, \mathrm{d}\beta \tag{13}$$

and an upper cutoff error

$$\mathcal{E}_U \sim \int_U^\infty \int_U^\infty f_U(\alpha) f_U(\beta) \left[\frac{(2l+3)\alpha\beta}{\zeta^{l+5/2}} + G_U(\zeta) - \frac{E}{\zeta^{l+3/2}} \right] \mathrm{d}\alpha\, \mathrm{d}\beta \tag{14}$$

where $f_L(x)$ and $G_L(x)$ are the limiting forms of $f(x)$ and $G(x)$ for small x and $f_U(x)$ and $G_U(x)$ are the limiting forms for large x. These are listed in Table 1 for each of the orbitals that we will consider.

Table 1. Limiting Behavior of $f(\alpha)$ and $G(\zeta)$ for Orbitals

orbital	$f_L(\alpha)$	$f_U(\alpha)$	$G_L(\zeta)$	$G_U(\zeta)$
Dawson	1	$\alpha^{-3/2}$	$\zeta^{-1/2}$	ζ^{-1}
Lorentzian	1	$\exp(-\alpha)$	$\zeta^{-1/2}$	$\zeta^{-3/2}$
Sech	$\exp(-1/(4\alpha))$	$\exp(-(\pi^2/4)\alpha)$	ζ^{-1}	$\zeta^{-3/2}$
Expo (1s)	$\exp(-1/(4\alpha))$	$\alpha^{-3/2}$	ζ^{-1}	ζ^{-1}
Expo (2s)	$\exp(-1/(16\alpha))$	$\alpha^{-3/2}$	ζ^{-1}	ζ^{-1}
Expo (3s)	$\exp(-1/(36\alpha))$	$\alpha^{-3/2}$	ζ^{-1}	ζ^{-1}
Expo (2p)	$\exp(-1/(16\alpha))$	$\alpha^{-3/2}$	ζ^{-2}	ζ^{-2}
Expo (3d)	$\exp(-1/(36\alpha))$	$\alpha^{-3/2}$	ζ^{-3}	ζ^{-3}

2.3. Discretization Error. In terms of the log exponents $s = \ln \alpha$ and $t = \ln \beta$, the energy error functional (eq 6) can be written

$$\mathcal{E} = \int_{-\infty}^\infty \int_{-\infty}^\infty F(\mathrm{e}^s, \mathrm{e}^t) \mathrm{e}^{s+t}\, \mathrm{d}s\, \mathrm{d}t \tag{15}$$

and adopting an infinite *even-tempered* Gaussian basis corresponds to approximating eq 15 by the quadrature

$$\mathcal{E} \approx h^2 \sum_{j=-\infty}^\infty \sum_{k=-\infty}^\infty F(\mathrm{e}^{jh}, \mathrm{e}^{kh}) \mathrm{e}^{(j+k)h} \tag{16}$$

Using the Fourier representation of the Dirac comb[49]

$$\Delta_h(z) = \frac{1}{h} \sum_{m=0}^\infty \cos\left[\frac{2m\pi z}{h} \right] \tag{17}$$

one can write the discretization error as

$$\begin{aligned} \mathcal{E}_D &= h^2 \sum_{j=-\infty}^\infty \sum_{k=-\infty}^\infty F(\mathrm{e}^{jh}, \mathrm{e}^{kh}) \mathrm{e}^{(j+k)h} - \mathcal{E} \\ &= h^2 \int_{-\infty}^\infty \int_{-\infty}^\infty F(\mathrm{e}^s, \mathrm{e}^t) \mathrm{e}^{s+t}\, \Delta_h(s)\, \Delta_h(t)\, \mathrm{d}s\, \mathrm{d}t - \mathcal{E} \\ &= \int_{-\infty}^\infty \int_{-\infty}^\infty F(\mathrm{e}^s, \mathrm{e}^t) \mathrm{e}^{s+t} \sum_{j=1}^\infty \sum_{k=1}^\infty \cos\left[\frac{2j\pi s}{h} \right] \\ &\quad \cos\left[\frac{2k\pi t}{h} \right] \mathrm{d}s\, \mathrm{d}t \end{aligned} \tag{18}$$

dx.doi.org/10.1021/ct300559t | J. Chem. Theory Comput. 2012, 8, 4891−4898

If F decays rapidly for large $|s|$ and $|t|$, the leading term in the double sum dominates, and by back-transforming to exponent variables, we obtain the Kutzelnigg expression

$$\mathcal{E}_D \sim \int_0^\infty \int_0^\infty F(\alpha, \beta) \cos\left[\frac{2\pi \ln \alpha}{h}\right] \cos\left[\frac{2\pi \ln \beta}{h}\right] \mathrm{d}\alpha\ \mathrm{d}\beta \tag{19}$$

If we move to polar coordinates, and assume that h is small, this becomes

$$\mathcal{E}_D \sim \int_0^\infty \int_0^{\pi/2} \frac{r}{2} F(r \sin\theta, r \cos\theta) \tan^{2i\pi/h}\theta\ \mathrm{d}\theta\ \mathrm{d}r \tag{20}$$

and, for many orbitals, the discretization error decays quickly as the even-tempering distance h is decreased.

3. CONVERGENCE OF FOUR ORBITAL TYPES

For many orbitals, we find that the lower cutoff error decays either algebraically ($\mathcal{E}_L \sim L^p$) or exponentially ($\mathcal{E}_L \sim \exp(-1)/(pL)$) with the smallest Gaussian exponent L and, analogously, the upper cutoff error decays either algebraically ($\mathcal{E}_U \sim U^{-q}$) or exponentially ($\mathcal{E}_U \sim \exp(-qU)$) with the largest Gaussian exponent U. The discretization error is often $\mathcal{E}_D \sim \exp(-2\pi^2/h)$, and we will assume that this is the case for all of the orbitals that we will consider.

We now examine the four model cases that result in these situations, using the even-tempered relationship

$$nh = \ln(U/L) \tag{21}$$

For clarity, and because we are principally interested in the qualitative behavior of the energy convergence, we assume unit coefficients throughout. Our asymptotic predictions are unaffected by this assumption.

Type A. If $\mathcal{E}_L$ is algebraic and $\mathcal{E}_U$ is algebraic, we have

$$\mathcal{E} = L^p + U^{-q} + \exp(-2\pi^2/h) \tag{22}$$

In the special case where $p = q$, minimization of $\mathcal{E}$ with respect to L and U leads to

$$LU = 1 \tag{23a}$$

$$2p \ln U \exp(-p \ln U) = \frac{n\pi^2}{\ln U} \exp\left[-\frac{n\pi^2}{\ln U}\right] \tag{23b}$$

and, for large n, these equations yield

$$L \sim \exp(-\pi\sqrt{n/p}) \tag{24a}$$

$$U \sim \exp(+\pi\sqrt{n/p}) \tag{24b}$$

$$\mathcal{E} \sim \exp(-\pi\sqrt{np}) \tag{24c}$$

Equation 24c predicts root-exponential convergence.

Type B. If $\mathcal{E}_L$ is algebraic and $\mathcal{E}_U$ is exponential, we have

$$\mathcal{E} = L^p + \exp(-qU) + \exp(-2\pi^2/h) \tag{25}$$

Minimization of $\mathcal{E}$ with respect to L and U leads to

$$L = (qU/p)^{1/p} \exp(-qU/p) \tag{26a}$$

$$qU \exp(-qU) = \frac{2n\pi^2}{\ln^2(U/L)} \exp\left[-\frac{2n\pi^2}{\ln(U/L)}\right] \tag{26b}$$

and, for large n, these equations yield

$$L \sim \exp(-\pi\sqrt{2n/p}) \tag{27a}$$

$$U \sim \pi\sqrt{2np}/q \tag{27b}$$

$$\mathcal{E} \sim \exp(-\pi\sqrt{2np}) \tag{27c}$$

Equation 27c predicts root-exponential convergence that is twice as fast as that in case A.

Type C. If $\mathcal{E}_L$ is exponential and $\mathcal{E}_U$ is algebraic, we have

$$\mathcal{E} = \exp(-1/(pL)) + U^{-q} + \exp(-2\pi^2/h) \tag{28}$$

Minimization of $\mathcal{E}$ with respect to L and U leads to

$$U = (pqL)^{1/q} \exp(1/(pqL)) \tag{29a}$$

$$\frac{1}{pL} \exp\left(-\frac{1}{pL}\right) = \frac{2n\pi^2}{\ln^2(U/L)} \exp\left[-\frac{2n\pi^2}{\ln(U/L)}\right] \tag{29b}$$

and, for large n, these equations yield

$$L \sim \frac{1}{\pi p\sqrt{2nq}} \tag{30a}$$

$$U \sim \exp(\pi\sqrt{2n/q}) \tag{30b}$$

$$\mathcal{E} \sim \exp(-\pi\sqrt{2nq}) \tag{30c}$$

Equation 30c predicts root-exponential convergence that is comparable to that in case B.

Type D. If $\mathcal{E}_L$ is exponential and $\mathcal{E}_U$ is exponential, we have

$$\mathcal{E} = \exp(-1/(pL)) + \exp(-qU) + \exp(-2\pi^2/h) \tag{31}$$

Minimization of $\mathcal{E}$ with respect to L and U leads to

$$pqLU = 1 \tag{32a}$$

$$qU \exp(-qU) = \frac{2n\pi^2}{\ln^2(pqU^2)} \exp\left[-\frac{2n\pi^2}{\ln(pqU^2)}\right] \tag{32b}$$

and, for large n, these equations yield

$$L \sim \frac{W(n\pi^2\sqrt{p/q})}{n\pi^2 p} \tag{33a}$$

$$U \sim \frac{n\pi^2/q}{W(n\pi^2\sqrt{p/q})} \tag{33b}$$

$$\mathcal{E} \sim \exp\left[-\frac{n\pi^2}{W(n\pi^2\sqrt{p/q})}\right] \tag{33c}$$

where W is the Lambert W function[28] or product log. Because $W(x)$ is almost flat for large x, eq 33c predicts that the energies of optimized Gaussian expansions of type D orbitals will converge only slightly slower than exponentially.

4. MODEL ORBITALS

We begin by considering four radial potentials $V(r)$ whose ground-state wave functions $\psi(r)$, and their Gaussian transforms $f(\alpha)$, can be found in closed form.

The optimal n-Gaussian approximation (1) has energy

$$E_n = \min_{c,a} \frac{\mathbf{c}^\dagger(\mathbf{T} + \mathbf{V})\mathbf{c}}{\mathbf{c}^\dagger \mathbf{S}\mathbf{c}} \tag{34}$$

Table 2. Even-Tempered Minimum (z_1) and Maximum (z_n) Log Exponents and Log Error ($\ln \varepsilon_n$) for the Energy-Optimized n-Term Gaussian Expansions of the Dawson, Lorentzian, Exponential, and Sech Orbitals

	Dawson			Lorentzian			Exponential			Sech		
n	z_1	z_n	$-\ln \varepsilon_n$	z_1	z_n	$-\ln \varepsilon_n$	z_1	z_n	$-\ln \varepsilon_n$	z_1	z_n	$-\ln \varepsilon_n$
1				−1.54	−1.54	2.34	−1.26	−1.26	2.58	−1.35	−1.35	3.61
2				−2.47	−0.25	4.36	−1.60	+0.29	4.26	−1.95	−0.56	6.74
3	−2.68	+1.62	4.20	−3.39	+0.10	5.68	−1.81	+1.36	5.48	−2.32	−0.11	9.80
4	−3.40	+2.31	5.14	−4.17	+0.35	6.98	−2.00	+2.21	6.69	−2.60	+0.19	12.8
5	−3.91	+3.02	5.99	−4.89	+0.53	8.08	−2.14	+2.96	7.73	−2.82	+0.43	15.7
6	−4.43	+3.60	6.79	−5.54	+0.67	9.13	−2.26	+3.64	8.74	−3.00	+0.63	17.7
7	−4.88	+4.15	7.53	−6.16	+0.79	10.1	−2.40	+3.27	9.68	−3.16	+0.78	20.0
8	−5.35	+4.61	8.21	−6.75	+0.89	11.0	−2.45	+4.87	10.6	−3.31	+0.93	22.0
9	−5.76	+5.07	8.85	−7.30	+0.98	11.9	−2.52	+5.43	11.4	−3.44	+1.05	24.3
10	−6.16	+5.48	9.46	−7.83	+1.05	12.7	−2.59	+5.97	12.2	−3.57	+1.18	26.6

Table 3. Fully Optimized Minimum (z_1) and Maximum (z_n) Log Exponents and Log Error ($\ln \varepsilon_n$) for the Energy-Optimized n-Term Gaussian Expansions of the Dawson, Lorentzian, Exponential, and Sech Orbitals

	Dawson			Lorentzian			Exponential			Sech		
n	z_1	z_n	$-\ln \varepsilon_n$	z_1	z_n	$-\ln \varepsilon_n$	z_1	z_n	$-\ln \varepsilon_n$	z_1	z_n	$-\ln \varepsilon_n$
1				−1.54	−1.54	2.34	−1.26	−1.26	2.58	−1.35	−1.35	3.61
2				−2.47	−0.25	4.36	−1.60	+0.29	4.26	−1.95	−0.56	6.74
3	−2.86	+1.53	4.26	−3.57	+0.20	6.10	−1.89	+1.50	5.80	−2.34	−0.12	9.82
4	−3.49	+2.44	5.36	−4.59	+0.48	7.64	−2.10	+2.56	7.23	−2.61	+0.18	12.8
5	−4.12	+3.21	6.37	−5.53	+0.68	9.04	−2.27	+3.53	8.57	−2.82	+0.42	15.7
6	−4.74	+3.89	7.30	−6.41	+0.84	10.3	−2.41	+4.42	9.82	−2.99	+0.60	18.6
7	−5.32	+4.52	8.18	−7.23	+0.97	11.5	−2.52	+5.25	11.0	−3.14	+0.76	21.4
8	−5.88	+5.11	9.00	−8.02	+1.08	12.7	−2.62	+6.04	12.1	−3.26	+0.89	24.1
9	−6.41	+5.67	9.79	−8.76	+1.18	13.8	−2.70	+6.78	13.2	−3.37	+1.01	26.8
10	−6.92	+6.20	10.5	−9.48	+1.26	14.8	−2.77	+7.49	14.2	−3.47	+1.11	29.5

Table 4. Fully Optimized Minimum (z_1) and Maximum (z_n) Log Exponents and Log Error ($\ln \varepsilon_n$) for the Energy-Optimized n-Term Gaussian Expansions of the 2s, 3s, 2p, and 3d Exponential Orbitals

	2s orbital			3s orbital			2p orbital			3d orbital		
n	z_1	z_n	$-\ln \varepsilon_n$	z_1	z_n	$-\ln \varepsilon_n$	z_1	z_n	$-\ln \varepsilon_n$	z_1	z_n	$-\ln \varepsilon_n$
1							−3.10	−3.10	4.44	−4.21	−4.21	5.57
2	−4.12	−1.14	4.81				−3.43	−1.97	6.37	−4.54	−3.31	7.65
3	−3.95	+0.52	6.62	−5.31	−1.14	5.99	−3.70	−1.09	8.21	−4.79	−2.59	9.67
4	−3.90	+1.87	7.90	−5.29	+0.48	7.86	−3.90	−0.31	9.94	−4.98	−1.96	11.6
5	−3.89	+3.12	8.44	−5.30	+1.79	9.50	−4.06	+0.40	11.6	−5.13	−1.39	13.4
6	−4.47	+2.93	9.91	−5.30	+2.95	10.8	−4.18	+1.05	13.1	−5.25	−0.86	15.2
7	−4.42	+3.96	11.3	−5.31	+4.03	11.5	−4.29	+1.67	14.6	−5.35	−0.35	16.9
8	−4.39	+4.92	12.6	−6.13	+4.06	12.1	−4.38	+2.25	16.0	−5.44	+0.12	18.4
9	−4.38	+5.84	13.6	−6.15	+5.11	12.5	−4.46	+2.81	17.3	−5.52	+0.58	20.0
10	−4.38	+6.72	14.2	−5.64	+4.90	13.9	−4.54	+3.34	18.6	−5.58	+1.01	21.5

where $\mathbf{c}^\dagger = (c_1,...,c_n)$ and the elements of the **S**, **T**, and **V** matrices are indicated in eqs 9 and 10.

Using the FindMinimum function in MATHEMATICA[50] to find the optimal c_k and α_k (for $n = 1, ..., 10$) for each potential, and bootstrapping from small to large n, we believe that we found the global minimum in each case.

The results allow us to study the behavior of ε_n with n for each orbital and can be compared with the predictions of the Kutzelnigg analysis. Table 2 reports results for 1s-type orbitals under the constraint of even-tempered exponents. Table 3 presents the corresponding results where the exponents are unconstrained. Table 4 gives results for the 2s, 3s, 2p, and 3d exponential orbitals.

4.1. The Dawson Orbital. The orbital

$$\psi_A(r) = 1 - \sqrt{\pi} r \exp(r^2) \operatorname{erfc}(r) \tag{35}$$

is the lowest eigenfunction of the potential

$$V_A(r) = \frac{1}{r^2}\left(1 + 5r^2 + 2r^4 - \frac{1 + r^2}{\psi_A(r)}\right) \tag{36}$$

and has energy $E = 0$. It has a cusp at $r = 0$ and decays slowly, so its exponent distribution

$$f_A(\alpha) = \frac{1}{2(1 + \alpha)^{3/2}} \tag{37}$$

attaches importance to the full range of exponents. The log-exponent distribution (Figure 2)

dx.doi.org/10.1021/ct300559t | J. Chem. Theory Comput. 2012, 8, 4891−4898

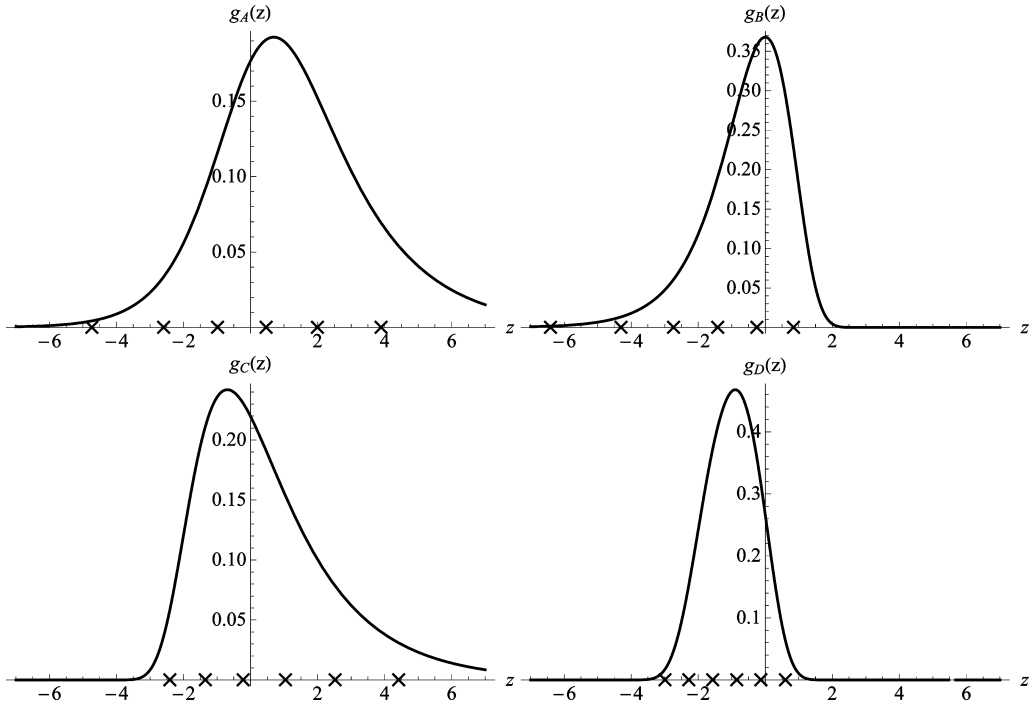

Figure 2. The log-exponent distributions for the Dawson (upper left), Lorentzian (upper right), exponential (lower left), and Sech (lower right) orbitals. Crosses indicate the z_i in the fully optimized six-term Gaussian expansion of each orbital.

$$g_A(z) \sim \begin{cases} \exp(+z) & z \to -\infty \\ \exp(-z/2) & z \to +\infty \end{cases} \tag{38}$$

decays slowly in both directions, and the spacing of the optimal z_i therefore increases to the left and the right. The importance of both small and large exponents is confirmed by the large negative z_n values in column 2 and the large positive z_n values in column 3 of Tables 2 and 3.

It can be shown from Table 1 that this is a type A orbital with $p = 3/2$, and the energy errors in column 4 therefore decay as $\exp(-\pi(3n/2)^{1/2})$.

4.2. The Lorentzian Orbital. The orbital

$$\psi_B(r) = \frac{1}{1 + r^2} \tag{39}$$

is the lowest eigenfunction of the potential

$$V_B(r) = \frac{1}{1 + r^2} - \frac{4}{(1 + r^2)^2} \tag{40}$$

and has energy $E = 0$. It has no cusp at $r = 0$ but decays slowly, so its exponent distribution

$$f_B(\alpha) = \exp(-\alpha) \tag{41}$$

emphasizes small exponents but not large ones. The log-exponent distribution (Figure 2)

$$g_B(z) \sim \begin{cases} \exp(+z) & z \to -\infty \\ \exp(-e^z) & z \to +\infty \end{cases} \tag{42}$$

is strongly negatively skewed, and as a result, the spacing of the optimal z_i increases to the left. The importance of Gaussians with small exponents is confirmed by the large negative z_1 values in column 5 of Tables 2 and 3.

It can be shown from Table 1 that this is a type B orbital with $p = 3/2$ and $q = 2$, and the energy errors in column 7 therefore decay as $\exp(-\pi(3n)^{1/2})$.

4.3. The Exponential orbital. The orbital

$$\psi_C(r) = \exp(-r) \tag{43}$$

is the lowest eigenfunction of the Coulomb potential

$$V_C(r) = -\frac{1}{r} \tag{44}$$

and has energy $E = -1/2$. It has a cusp at $r = 0$ but decays rapidly at large r, so its exponent distribution

$$f_C(\alpha) = \frac{1}{\sqrt{4\pi\alpha^3}} \exp\left(-\frac{1}{4\alpha}\right) \tag{45}$$

emphasizes large exponents but not small ones. The log-exponent distribution (Figure 2)

$$g_C(z) \sim \begin{cases} \exp(-e^{-z}/4) & z \to -\infty \\ \exp(-z/2) & z \to +\infty \end{cases} \tag{46}$$

is strongly positively skewed, and as a result, the spacing of the optimal z_i increases to the right. The importance of Gaussians with large exponents is confirmed by the large positive z_n values in column 9 of Tables 2 and 3.

It can be shown from Table 1 that this is a type C orbital with $p = 2$ and $q = 3/2$, and as Kutzelnigg found, the energy errors in column 9 therefore decay as $\exp(-\pi(3n)^{1/2})$. They are, in fact, similar to the Lorentzian energy errors, albeit for complementary reasons.

4.4. The Sech Orbital. The orbital

$$\psi_D(r) = \operatorname{sech} r \tag{47}$$

is the lowest eigenfunction of the potential[51]

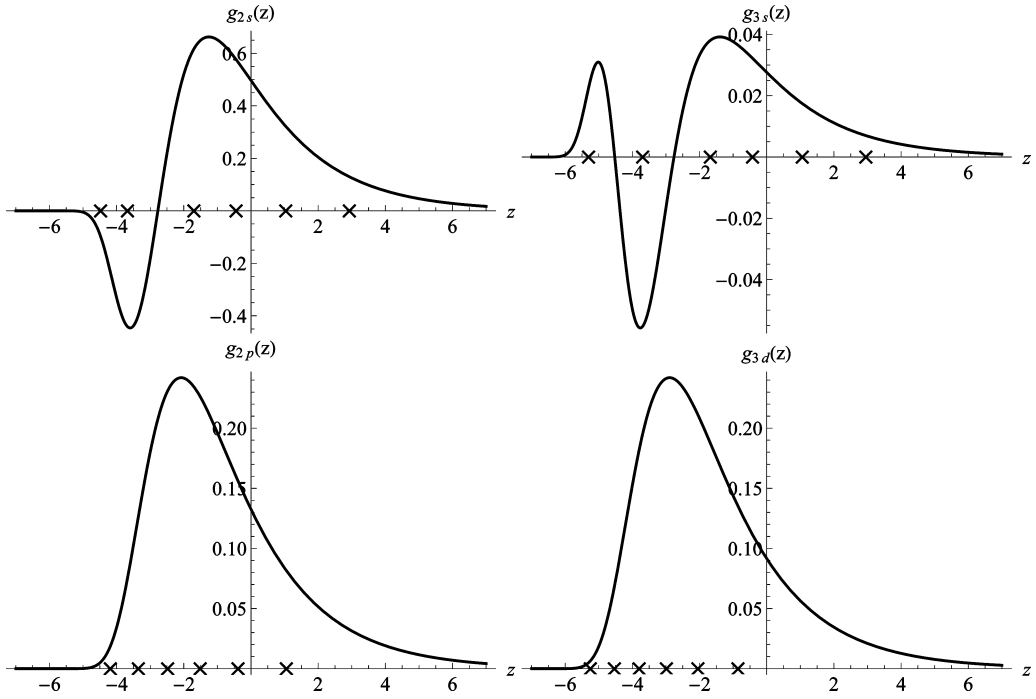

Figure 3. The log-exponent distributions for the 2s (upper left), 3s (upper right), 2p (lower left), and 3d (lower right) exponential orbitals. Crosses indicate the z_i in the fully optimized six-term Gaussian expansion of each orbital.

$$V_{\mathrm{D}}(r) = -\mathrm{sech}^2 r - \frac{\tanh r}{r} \tag{48}$$

and has energy $E = -1/2$. It has no cusp at $r = 0$ and decays rapidly at large r, so its exponent distribution

$$f_{\mathrm{D}}(\alpha) = \frac{1}{\sqrt{4\pi\alpha^3}}\theta'_1(0, \mathrm{e}^{-1/\alpha}) \tag{49}$$

(where θ_1 is an elliptic theta function[28]) attaches little significance to either small or large exponents. The log-exponent distribution (Figure 2)

$$g_{\mathrm{D}}(z) \sim \begin{cases} \exp(-\mathrm{e}^{-z}/4) & z \to -\infty \\ \exp(-\pi^2\mathrm{e}^{z}/4) & z \to +\infty \end{cases} \tag{50}$$

is both strongly localized and highly symmetrical, so the optimal z_i are tightly packed and almost uniformly spaced. It is not surprising that even-tempered Gaussian basis sets perform particularly well for this orbital. Because of the unimportance of both small and large exponents, the z_1 and z_n values in columns 11 and 12 of Tables 2 and 3 grow only slowly with n.

It follows from Table 1 that this is a type D orbital with $p = 2$ and $q = \pi^2/2$, and the energy errors in the last column of the tables therefore decay much more rapidly than in the Lorentzian and exponential cases.

5. HIGHER EXPONENTIAL ORBITALS

We now consider four more orbitals, extending our analysis to higher eigenfunctions of the hydrogen atom. Using Table 1, it can be shown that all of these are type C orbitals, but with varying p and q parameters.

5.1. The 2s Orbital. The orbital

$$\psi_{2\mathrm{s}}(r) = (2 - r)\exp(-r/2) \tag{51}$$

is the second s-type eigenfunction of the Coulomb potential and has energy $E = -1/8$. It has a cusp at $r = 0$ but decays rapidly at large r, so its exponent distribution

$$f_{2\mathrm{s}}(\alpha) = \frac{16\alpha - 1}{16\sqrt{\pi\alpha^5}}\exp\left(-\frac{1}{16\alpha}\right) \tag{52}$$

emphasizes large exponents. The optimal exponents cluster to the left and right of the node at $\alpha = 1/16$, and this is illustrated by the $n = 6$ exponents shown in Figure 3. As for the 1s orbital, the log-exponent distribution (Figure 3)

$$g_{2\mathrm{s}}(z) \sim \begin{cases} \exp(-\mathrm{e}^{-z}/16) & z \to -\infty \\ \exp(-z/2) & z \to +\infty \end{cases} \tag{53}$$

is positively skewed and the spacing of the optimal z_i consequently increases to the right. The importance of large Gaussian exponents is confirmed by the large positive z_n values in column 3 of Table 4.

This orbital has $p = 8$ and $q = 3/2$, and the energy errors in column 4 of Table 4 therefore decay as $\exp(-\pi(3n)^{1/2})$. By comparing columns 2 and 4 of Table 4 with columns 8 and 10 of Table 3, we see that the smallest exponents for the 2s orbital are much smaller than those for the 1s orbital, but that the energy errors are similar. These observations are consistent with eq 30, which shows that p affects the low exponents, but that the high exponents and the error depend only on q.

5.2. The 3s Orbital. The orbital

$$\psi_{3\mathrm{s}}(r) = (27 - 18r + 2r^2)\exp(-r/3) \tag{54}$$

is the third s-type eigenfunction of the Coulomb potential and has energy $E = -1/18$. It has a cusp at $r = 0$ but decays rapidly at large r, so its exponent distribution

$$f_{3\mathrm{s}}(\alpha) = \frac{1458\alpha^2 - 108\alpha + 1}{108\sqrt{\pi\alpha^7}}\exp\left(-\frac{1}{36\alpha}\right) \tag{55}$$

dx.doi.org/10.1021/ct300559t | J. Chem. Theory Comput. 2012, 8, 4891−4898

emphasizes large exponents. As for the 1s and 2s orbitals, the log-exponent distribution (Figure 3)

$$g_{3s}(z) \sim \begin{cases} \exp(-e^{-z}/36) & z \to -\infty \\ \exp(-z/2) & z \to +\infty \end{cases} \quad (56)$$

is positively skewed and the spacing of the optimal exponents increases to the right. The importance of large exponents is confirmed by the large positive z_n values in column 6 of Table 4.

This orbital has $p = 18$ and $q = 3/2$, and the energy errors in column 7 of Table 4 therefore decay as $\exp(-\pi(3n)^{1/2})$. Comparison of columns 2 and 5 of Table 4 reveals that the smallest exponents for the 3s orbital are even smaller than those for the 2s orbital, but that the energy errors are similar. As above, these observations are consistent with eq 30.

5.3. The 2p Orbital. The orbital

$$\psi_{2p}(r) = r \exp(-r/2) \quad (57)$$

is the radial part of the lowest p-type eigenfunction of the Coulomb potential and has energy $E = -1/8$. It decays rapidly at large r but has only a second-order cusp at $r = 0$, so its exponent distribution

$$f_{2p}(\alpha) = \frac{1}{\sqrt{16\pi\alpha^3}} \exp\left(-\frac{1}{16\alpha}\right) \quad (58)$$

favors smaller exponents than the 2s orbital. The log-exponent distribution (Figure 3)

$$g_{2p}(z) \sim \begin{cases} \exp(-e^{-z}/16) & z \to -\infty \\ \exp(-z/2) & z \to +\infty \end{cases} \quad (59)$$

is strongly positively skewed, and as a result, the spacing of the optimal z_i increases to the right. The importance of Gaussians with large exponents is confirmed by the large positive z_n values in column 3 of Table 4.

This orbital has $p = 8$ and $q = 5/2$, and the energy errors in column 4 of Table 4 therefore decay as $\exp(-\pi(5n)^{1/2})$, which is significantly faster than those for the 2s orbital.

5.4. The 3d Orbital. The orbital

$$\psi_{3d}(r) = r^2 \exp(-r/3) \quad (60)$$

is the radial part of the lowest d-type eigenfunction of the Coulomb potential and has energy $E = -1/18$. It decays rapidly at large r but has only a third-order cusp at $r = 0$, so its exponent distribution

$$f_{3d}(\alpha) = \frac{1}{\sqrt{36\pi\alpha^3}} \exp\left(-\frac{1}{36\alpha}\right) \quad (61)$$

favors even smaller exponents than the 2p orbital. The log-exponent distribution (Figure 3)

$$g_{3d}(z) \sim \begin{cases} \exp(-e^{-z}/36) & z \to -\infty \\ \exp(-z/2) & z \to +\infty \end{cases} \quad (62)$$

is strongly positively skewed, and as a result, the spacing of the optimal z_i increases to the right. The importance of Gaussians with large exponents is confirmed by the large positive z_n values in column 6 of Table 4.

This orbital has $p = 18$ and $q = 7/2$, and the energy errors in the final column of Table 4 therefore decay as $\exp(-\pi(7n)^{1/2})$, which is even faster than those for the 2p orbital.

6. CONCLUDING REMARKS

In the Introduction to this paper, we asked whether the root-exponential convergence of the Gaussian expansion of the exponential orbital stems from its cusp at $r = 0$ or its cusp at $r = \infty$. The rapid convergence observed for the Sech orbital, which lacks the first cusp but has the second, allows us unambiguously to conclude that the slower convergence of the exponential is due to the cusp at $r = 0$.

The discovery that 2s and 3s orbitals exhibit the same convergence behavior as the 1s orbital leads us to conclude that their analysis gives insight into the Gaussian convergence behavior in *any* molecular orbital that possesses first-order cusps at the nuclei.

We found that the Gaussian expansions of hydrogenic orbitals with higher angular momentum (e.g., 2p and 3d) also converge root-exponentially. Again, this can be traced to their cusps at $r = 0$, but because an orbital with angular momentum l has an $(l + 1)$-th order cusp, the convergence rate grows with l. Specifically, we find that the error decays asymptotically as $\exp(-\pi((2l + 3)n)^{1/2})$.

Our numerical studies of both even-tempered and fully optimized basis sets produced reassuringly similar results and give us confidence that analysis of even-tempered basis sets provides reliable insights into the behavior of fully optimized basis sets.

Replacing a point nucleus with a finite-sized nucleus, as is often done in relativistic calculations, would eliminate the first-order cusp in the exact wave function, improving convergence, but higher-order cusps would still exist and thus root-exponential convergence would be observed.

Finally, we observe that the inability of Gaussian to model nuclear-electron cusps in molecular orbitals causes Gaussian basis sets to be much larger than they would otherwise need to be. This frustrating effect, which causes many of the Gaussian exponents to become very large (see column 9 of Table 3), is one the primary motivations for the use of pseudopotentials in quantum chemistry and molecular physics.

AUTHOR INFORMATION

Corresponding Author

*E-mail: laura.mckemmish@gmail.com; peter.gill@anu.edu.au.

Notes

The authors declare no competing financial interest.

ACKNOWLEDGMENTS

P.M.W.G. thanks the ARC for funding (Grants DP1094170 and DP120104740).

REFERENCES

(1) Hehre, W. J.; Radom, L.; Schleyer, P.; Pople, J. A. *Ab Initio Molecular Orbital Theory*; John Wiley & Sons Inc: New York, 1986; pp 5−16.

(2) Szabo, A.; Ostlund, N. S. *Modern Quantum Chemistry*; McGraw-Hill: New York, 1989; pp 108−229.

(3) Parr, R. G.; Yang, W. *Density-Functional Theory of Atoms and Molecules*; Oxford: Clarendon Press, 1989; pp 142−149.

(4) Jensen, F. *Introduction to Computational Chemistry*; Wiley: New York, 1999; pp 53−97; 347−353.

(5) Woodward, R. B.; Hoffmann, R. *J. Am. Chem. Soc.* **1965**, *87*, 395−397.
(6) Fleming, I. *Frontier Orbitals and Organic Chemical Reactions*; Wiley: Chichester, U. K., 1976; pp 5−32.
(7) Smith, M.; March, J. *March's Advanced Organic Chemistry: Reactions, Mechanisms, and Structure*, 6th ed.; McGraw-Hill: Tokyo, 2007; pp 3−103.
(8) Cotton, F. A.; Wilkinson, G. *Advanced Inorganic Chemistry*; Wiley Interscience: New York, 1999; pp 629−657.
(9) Gerloch, M. *Magnetism and Ligand-Field Analysis*; Cambridge University Press: Cambridge, U. K., 2009; pp 3−35.
(10) Roothaan, C. C. J. *Rev. Mod. Phys.* **1951**, *23*, 69−89.
(11) Hall, G. G. *Proc. R. Soc. London* **1951**, *A205*, 541−552.
(12) Boys, S. F. *Proc. R. Soc. London* **1950**, *A200*, 542−554.
(13) Dupuis, M.; Rys, J.; King, H. F. *J. Chem. Phys.* **1976**, *65*, 111.
(14) Pople, J. A.; Hehre, W. J. *J. Comp. Phys* **1978**, *27*, 161.
(15) McMurchie, L. E.; Davidson, E. R. *J. Comput. Phys.* **1978**, *26*, 218.
(16) Obara, S.; Saika, A. *J. Chem. Phys.* **1986**, *84*, 3963.
(17) Head-Gordon, M.; Pople, J. A. *J. Chem. Phys.* **1988**, *89*, 5777.
(18) Gill, P. M. W.; Head-Gordon, M.; Pople, J. A. *J. Phys. Chem.* **1990**, *94*, 5564−5572.
(19) Gill, P. M. W.; Johnson, B. G.; Pople, J. A. *Int. J. Quantum Chem.* **1991**, *40*, 745−752.
(20) Gill, P. M. W. *Adv. Quantum Chem.* **1994**, *25*, 141−205.
(21) Gill, P. M. W.; Adamson, R. D. *Chem. Phys. Lett.* **1996**, *261*, 105−110.
(22) Adams, T. R.; Adamson, R. D.; Gill, P. M. W. *J. Chem. Phys.* **1997**, *107*, 124−131.
(23) Adamson, R. D.; Dombroski, J. P.; Gill, P. M. W. *J. Comput. Chem.* **1999**, *20*, 921−927.
(24) Fusti-Molnar, L.; Pulay, P. *J. Chem. Phys.* **2002**, *117*, 7827−7835.
(25) Komornicki, A.; King, H. F. *J. Chem. Phys.* **2011**, *134*, 244115.
(26) Hollett, J. W.; Gill, P. M. W. *Phys. Chem. Chem. Phys.* **2011**, *13*, 2972−2978.
(27) Limpanuparb, T.; Hollett, J. W.; Gill, P. M. W. *J. Chem. Phys.* **2012**, *136*, 104102.
(28) Olver, F. W. J.; Lozier, D. W.; Boisvert, R. F.; Clark, C. W. *NIST Handbook of Mathematical Functions*; Cambridge University Press: New York, 2010; pp 160−167.
(29) Lippert, G.; Hutter, J.; Parrinello, M. *Mol. Phys.* **1997**, *92*, 477−487.
(30) VandeVondele, J.; Krack, M.; Mohamed, F.; Parrinello, M.; Chassaing, T.; Hutter, J. *Comput. Phys. Commun.* **2005**, *358*, 103−128.
(31) Kato, T. *Comm. Pure. Appl. Math* **1957**, *10*, 151−177.
(32) Handy, N. C.; Marron, M. T.; Silverstone, H. J. *Phys. Rev.* **1969**, *180*, 45−48.
(33) Huzinaga, S. *J. Chem. Phys.* **1965**, *42*, 1293−1302.
(34) Boyd, J. P. *Chebyshev and Fourier Spectral Methods*, 2nd ed.; Dover: New York, 2000; pp 19−60; 98−108.
(35) Klopper, W.; Kutzelnigg, W. *THEOCHEM* **1986**, *135*, 339−356.
(36) Kutzelnigg, W. *Int. J. Quantum Chem.* **1994**, *51*, 447−463.
(37) Kutzelnigg, W. *Oberwolfach Reports* **2011**, *8*, 1775−1785.
(38) Kutzelnigg, W. *AIP Conf. Proc.* **2012**, in press.
(39) Kutzelnigg, W. *Int. J. Quantum Chem.* **2012**, in press.
(40) Schmidt, M. W.; Ruedenberg, K. *J. Chem. Phys.* **1979**, *71*, 3951−3962.
(41) Feller, D. F.; Ruedenberg, K. *Theor. Chim. Acta* **1979**, *52*, 231−251.
(42) Whittaker, E. T. *Proc. Roy. Soc. Edin.* **1915**, *35*, 181−194.
(43) Whittaker, J. M. *Interpolatory Function Theory*; Cambridge tracts in mathematics and mathematical physics 33; Cambridge University Press: London, 1935.
(44) Hehre, W. J.; Ditchfield, R.; Pople, J. A. *J. Chem. Phys.* **1972**, *56*, 2257−2261.
(45) Dunning, T. H. *J. Chem. Phys.* **1989**, *90*, 1007−1023.
(46) Jensen, F. *J. Chem. Phys.* **2001**, *115*, 9113−9125.
(47) The angular part of the wave function has no effect on the convergence behavior of the Gaussian expansion.
(48) The Gaussian representation can be found as the inverse Laplace transform of ψ, using r^2 as the transform variable.
(49) Cordoba, A. *Lett. Math. Phys.* **1989**, *17*, 191−196.
(50) *Mathematica*, version 8.0; Wolfram Research, Inc.: Champaign, IL, 2011.
(51) Gilbert, A. T. B.; Gill, P. M. W. *Chem. Phys. Lett.* **1999**, *312*, 511−521.